Exploratory Comparison of Human Rib Structural Behavior in Two Dynamic Loading Scenarios

Amanda M. Agnew, Akshara Sreedhar, John H. Bolte IV, Yun-Seok Kang

Abstract The objective of this study was to evaluate biomechanical response differences in human ribs subjected to simplified anterior-posterior (AP) dynamic loading versus AP loading combined with lateral (AP-L). Twelve bilateral pairs of 6th human ribs from an age-distributed sample (54 ± 17 years) were included in this study. One rib within each pair was selected to undergo 2D simplified AP loading to failure at 2 m/s. The other rib within the pair was tested in the same AP scenario, but with the added element of a rigid plate to constrain lateral displacement (AP-L). This set-up was intended to simply represent the combined AP and lateral loading the thorax would experience with a shoulder-belt pretensioner and a side airbag in a side impact. Results showed a significant response difference in time to fracture, displacement, peak force, and structural stiffness between AP only and AP-L tests. This work highlights the complexity of combined loading on human ribs that has not previously been investigated, and provides important evidence to explore variability in whole thoracic response and injury severities in various scenarios with different combinations of restraints in physical and simulated experiments.

Keywords Combined thoracic loading, frontal impact, rib fracture, side impact, thorax

I. INTRODUCTION

Post-mortem human subject (PMHS) testing has been accomplished in various test scenarios throughout recent history. Frontal hub impacts [1-3], bench top belt loading tests [4-8], and sled tests [9-14] have provided critical thoracic biomechanical response and injury risk data [15-16]. Lateral thoracic tests have been approached in a similar manner [17-19] utilizing hub impacts [20], airbag loading [21-22], and sled tests [23-26]. Oblique or offset testing was later explored to compare thoracic response and injuries to the more traditional data as it became more apparent that purely frontal or purely lateral impacts are not always realistic [27-31].

This progression of work was necessary in order to better understand thoracic response, injury mechanisms, and injury thresholds and has resulted in useful safety tools such as anthropomorphic test devices (ATDs) and computational human body models (HBMs). However, because of the necessarily simplistic approach in all experimental work to various degrees, the performance of ATDs and HBMs are generally optimized to be uni-directional. They are tested for biofidelity or validated, and equipped with instrumentation (i.e., ATDs) that is often restricted to one direction only, as they are meant to be used to evaluate the effects of frontal *or* side impacts, but rarely both simultaneously. As a result, some vehicle restraint systems are similarly optimized to be unidirectional; frontal airbags or side airbags deploy in frontal or side impacts, respectively. However, seatbelts are designed to couple vehicle occupants to their seat regardless of the crash direction.

Pretensioning belts hold the torso tightly in the seat from the shoulder retractor and/or the buckle, and will deploy in most crash modes, e.g., front, oblique, and side. Although it is accepted that tethering occupants into the seat increases their level of protection in a crash, it is still unclear whether a pretensioning belt may influence occupant injury risk in all crash modes. For instance, a near side impact crash would result in combined loading of the bony thorax whereby the pretensioning seatbelt would provide loading in an anterior-posterior (AP) direction while either door panel intrusion or a side airbag would provide lateral loading to the thorax on the struck side. Lateral thoracic deflection is an established injury criterion in side impacts [18][23][32], but the role of AP belt loading due to pretensioning remains unexplored in this context despite the realistic presence of a shoulder belt positioned on occupants in almost every real-world and simulated (experimental or computational) side impact crash scenario [33].

Most retrospective or experimental studies focus on the effects of either the restraints meant for protection

AM Agnew is an Associate Professor (amanda.agnew@osumc.edu, +1.614.366.2005), A Sreedhar is an MS student, JH Bolte IV is a Professor, and Y-S Kang is an Assistant Professor, Injury Biomechanics Research Center, The Ohio State University, Columbus, OH, USA.

in frontal crashes, i.e., belt with load limiters, steering wheel airbag [34], *or* the restraints meant for protection in side crashes independently [35], but rarely are the combined effects of these restraints considered, with a few exceptions [36-37]. While investigating thoracic biomechanical responses in small female PMHS' in a realistic side impact scenario, Shurtz et al. [38] found significant variation in the mechanism and timing of rib fracture occurrence relative to the different restraint interactions in these PMHS by using non-censored strain gauge data. They suggested future work focus on specifically exploring the effects of combined loading to the thorax [38], so their complex findings in concert with the general lack of knowledge in this area served as the main motivation for the current study. Similarly, while a plethora of whole rib dynamic biomechanical response and failure data exist for frontal loading [39-41], and although scarce, some data also exist for lateral loading [42], no whole rib experimental studies exist quantifying structural response to both frontal and lateral loading combined. Therefore, the objective of the current study was to identify biomechanical response differences in human ribs subjected to simplified anterior-posterior (AP) loading versus anterior-posterior loading with a lateral constraint (AP-L), in order to provide foundational evidence to instigate further exploration of combined loading in a more complex test scenario.

II. METHODS

Sample

Whole, excised ribs were isolated from tissue donors to The Ohio State University Body Donation Program or Lifeline of Ohio and stored at -20°C in normal saline soaked gauze. Twelve bilateral pairs of 6th human ribs from an age-distributed sample (54 ± 17 years) were included in this study. Ribs were chosen from individuals across the adult age spectrum (30-76 years) and such that males and females of similar age were represented in order to reduce the potential of an age or sex bias in the sample (Table I).

TABLE I
DEMOGRAPHICS & TEST MATRIX FOR RIB PAIRS

Pair	Age (yrs)	Sex	Height (cm)	Weight (cm)	Loading Condition	Rib Side
1	30	M	185	90	AP	R
					AP-L	L
2	30	F	168	77	AP	L
					AP-L	R
3	42	M	174	76	AP	L
					AP-L	R
4	43	F	173	89	AP	L
					AP-L	R
5	48	M	170	53	AP	R
					AP-L	L
6	47	F	163	76	AP	R
					AP-L	L
7	57	M	188	61	AP	L
					AP-L	R
8	57	F	163	50	AP	L
					AP-L	R
9	70	M	174	81	AP	R
					AP-L	L
10	72	F	168	41	AP	R
					AP-L	L
11	76	M	175	93	AP	L
					AP-L	R
12	76	F	160	68	AP	L
					AP-L	R

Experimental Testing

Based on previous work establishing symmetry between sides, it was assumed that ribs of the same level (i.e., 6th ribs) within pairs would exhibit similar properties [43-44]. Therefore, individual ribs within bilateral pairs were utilized for direct comparisons between two different loading conditions (Table I). One rib within each pair was randomly selected to undergo 2D simplified anterior-posterior (AP) loading to failure at 2m/s as has previously been described in detail elsewhere [39]. Instrumentation included a six-axis load cell (Humanetics, CRABI neck, IF-954, Plymouth, MI, USA) to record forces behind the vertebral rib end and a displacement potentiometer (AMETEK, Rayelco P-20A, Inc. Berwyn, PA, USA) to measure global displacement in the primary loading direction (-X) connected to the moving plate driving the sternal (anterior) rib end posteriorly (Fig. 1). Uni-axial strain gauges (CEA-06-062UW-350, Vishay Micro-Measurement, Shelton, CT, USA) were applied at four locations along the longitudinal axis of the rib; 30% and 60% of total rib curve length (Cv.Le; measured from the vertebral end) on the pleural and cutaneous surfaces.

The opposite side rib within each pair was tested in the same AP scenario, but with the added element of a stationary rigid aluminum plate to constrain lateral (Y) displacement (AP-L) and an additional six-axis load cell (Humanetics, Hybrid III 3 year lumbar, 2944JFL, Plymouth, MI, USA) above the plate (Fig. 2). The initial position of the plate was adjusted so each rib apex was just barely touching the plate, thereby not allowing for any lateral displacement (Y), i.e., bending, to occur during the event. This set-up was intended to simply approximate the combined anterior-posterior and lateral loading the thorax would experience with both a shoulder-belt pretensioner and a side airbag in a near-side impact crash. Peak force in X and Y directions, X displacement, structural stiffness (linear portion of F_X-D curve), and total energy (area under F_X-D curve) were calculated from Load Cell 1 for direct comparison between both loading scenarios as outlined in [39]. Peak force in X and Y were also calculated from Load Cell 2. All force and displacement data were filtered using Channel Frequency Class (CFC) 180 [45]. Fracture locations were documented relative to the total Curve Length (Cv.Le) of each rib as a normalized distance from the vertebral rib end. Additionally, strain data were observed raw to identify time of failure.

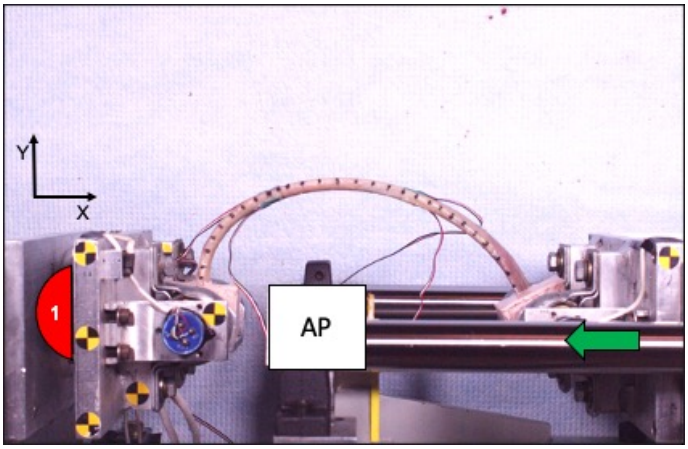

Fig. 1. Exemplar test set-up for AP loading condition (Left 6th rib from Pair 4) illustrating initial rib position (time zero) and Load Cell 1 posterior to the vertebral rib end.

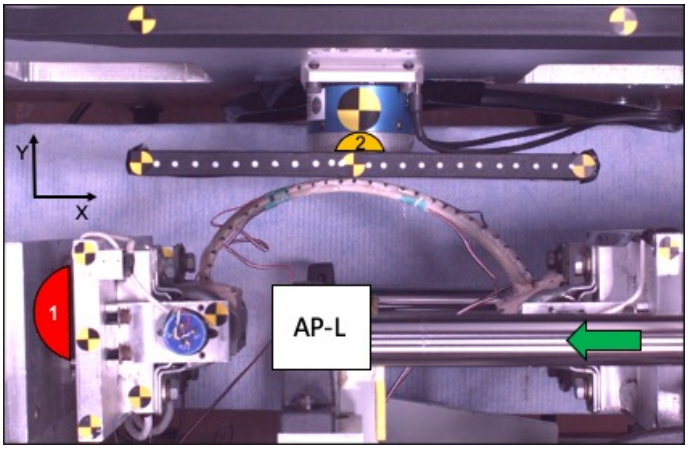

Fig. 2. Exemplar test set-up for AP-L loading condition (Right 6th rib from Pair 4) illustrating initial rib position (time zero) and Load Cell 1 as well as Load Cell 2 above the added rigid plate.

Data Analysis

For comparison of all properties between AP and AP-L conditions, percent differences were calculated as:

$$\frac{AP\ value - APL\ value}{0.5 \times (AP\ value + APL\ value)} \times 100 \quad (1)$$

Mann-Whitney tests were utilized to assess differences in medians between loading conditions. Alpha level was set to 0.05 to establish statistical significance.

III. RESULTS

Structural properties comparisons between loading conditions are included in Table II, including results of Mann-Whitney tests for differences in medians (Minitab®18 Statistical Software) between AP and AP-L tests. It is important to recall these properties were calculated utilizing the load cell behind the vertebral rib end that was present for both conditions (Load Cell 1, Figs. 1-2), allowing for direct comparisons. All ribs tested in combined loading (AP-L) were not free to bend laterally as they naturally would and, therefore, fractured earlier than those loaded in AP ($p<0.0001$). This resulted in significantly less displacement before failure in the AP-L tests ($p<0.0001$). Peak force in the primary loading direction (X) was significantly greater in the AP-L loaded ribs compared to the AP only ($p=0.004$). In combination with less displacement, the greater force magnitudes resulted in significantly greater structural stiffness ($p<0.0001$) for ribs in the AP-L tests. Qualitatively, these differences are apparent in all twelve pairs of F_X-D responses shown in Figs. A1-A12. For the AP tests in which all the ribs remained unconstrained laterally, not surprisingly, the peak force in Y was very low, but with the addition of the lateral constraint the peak force in Y was significantly greater ($p<0.0001$) with a median of 257N.

For the AP-L tests only, the load cell positioned above the rigid plate (Load Cell 2, Fig. 2) captured an average of 470N in the Y direction (SD=282N, range=198-1268) and only 62N in the X direction (SD=36N, range=30-160N), indicating the rigid plate did provide constraint as intended and that the friction as the rib slid posteriorly along the plate was minimal.

TABLE II
STRUCTURAL PROPERTY COMPARISONS FROM LOAD CELL 1

		Mean (SD)	Mean % Diff	Median	Diff Estimate	95% CI for Diff	p-value
Time of Fracture *(ms)*	AP	35.3 (11.6)	68.1	33.9	15.8	10.8, 21.1	<0.0001
	AP-L	17.4 (3.2)		17.1			
Displacement$_X$ *(%)*	AP	22.8 (10.3)	106.5	20.1	13.8	10.0, 17.9	<0.0001
	AP-L	7.0 (3.1)		6.9			
Peak Force$_X$ *(N)*	AP	110.2 (62.4)	-71.5	102.0	-88.3	-137.9, -40.9	0.004
	AP-L	232.9 (184.7)		188.2			
Peak Force$_Y$ *(N)*	AP	6.6 (3.5)	-190.9	6.2	-247.1	-313.4, -172.6	<0.0001
	AP-L	283.8 (160.3)		256.9			
Stiffness$_X$ *(N/mm)*	AP	3.5 (2.6)	-165.9	2.8	-26.5	-35.9, -19.0	<0.0001
	AP-L	37.2 (28.4)		29.7			
Total Energy$_X$ *(N*mm)*	AP	3387 (2384)	39.2*	2369	656	-627, 2635	0.237
	AP-L	2278 (1487)		2078			

*Mean % Diff of Total Energy included positive and negative values so should be interpreted with caution

Number and location of fractures were compared between AP and AP-L conditions (Table AI). As shown in Fig. 3, the range and median of fracture locations were not different between test conditions (Mann-Whitney, $p=0.90$). However, with the presence of the lateral plate, it was observed that no fractures occurred in the middle portion of ribs that were pushed against the plate. The distribution is split such that fractures clustered on either end of these ribs. Because there were so few ribs that sustained three fractures (Table AI), differences between number of fractures sustained in AP vs AP-L tests could only be assessed for one and two fractures, for which no significant associations were found (Chi-square, $p=0.46$).

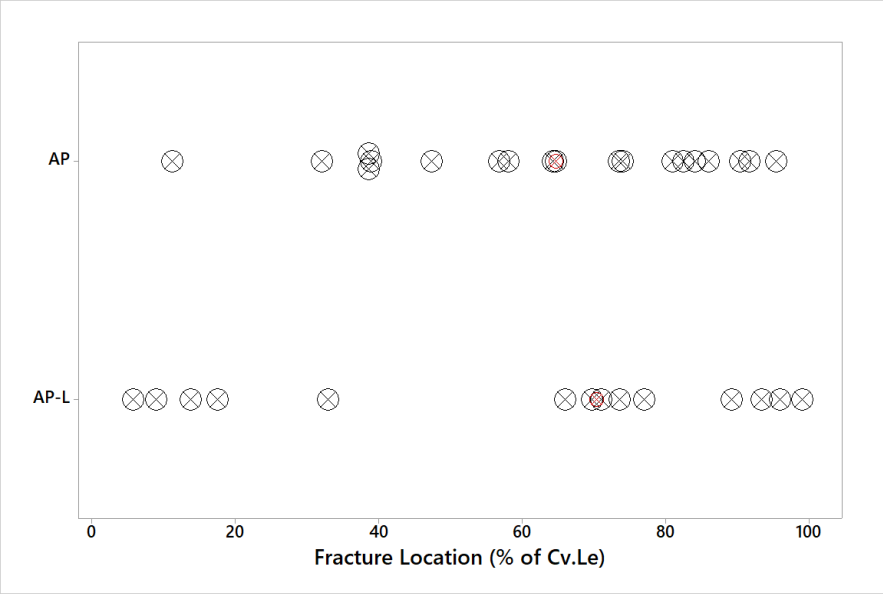

Fig. 3. Fracture location comparisons between AP and AP-L tests. Medians (indicated in red) for each sample were similar (Mann-Whitney, p=0.90).

IV. DISCUSSION

Three of the twelve rib pairs (Pairs 4, 9, and 10) exhibited behavior that allowed the rib to slide under the rigid plate in the primary loading direction (X) rather than to bend into the plate (Y) as was initially expected. Evidence for this can be seen in the F_X-D curves in Figs. A4, A9, and A10 where the force plateaued or even dropped considerably, as in Pairs 9 and 10, prior to actual failure. It is unknown if this is a phenomenon that could occur with AP loading and side restraint, e.g., from an airbag or even a door liner, in a more realistic scenario. It is also possible that the fracture timing established from a sharp drop in strain included error because 1) the gauges (applied at 30% and 60%) were sometimes very far from the fracture location (Fig. 3), and 2) if strains caused by addition of the lateral plate were off-axis the uni-axial gauges would not be sensitive in any other direction other than along the long axis of the rib in order to record this properly.

The duration (time to fracture) of the AP-L tests was approximately half that observed in AP tests (-49% difference, Table II). Similarly, the relative amount of displacement prior to fracture of AP-L tests ranged from only 3-13%, and was ~69% less than AP only tests. The quick failure with so little deflection could have serious implications for injury outcomes in more realistic PMHS tests and, therefore, real-world motor vehicle crashes based on timing of restraint system deployment. Specifically, during a crash event, if the pretensioner loaded the thorax (anterior-posterior) before the side airbag (lateral), there may be different injury outcomes than if the pretensioner and airbag deployed simultaneously. Additionally, existing thoracic injury predictors are based on rib deflection as developed by only considering frontal *or* side impact tests [17-18][24][46], with the underlying concept that injury occurs at greater deflection. However, the quick failure observed in the present study indicates that existing side injury criteria may benefit from reevaluation to incorporate the potential effects of frontal and lateral combined loading where injury occurs at low displacements and may be underestimating injuries. The phenomena of combined loading could also aid ATDs developed for omnidirectional uses rather than only frontal or side impacts. It is possible that updated injury risk curves should be developed for this particular scenario.

This study explored a scenario in which AP and lateral constraint were occurring together, but the differences may have been even more marked if AP loading and dynamic lateral loading (not simply static constraint) were occurring simultaneously. Holcombe et al. [47] investigated individual rib stiffness under these particular boundary conditions using finite element simulation and found that axial loading with a lateral constraint (our AP-L condition) resulted in higher rib stiffness than in free axial loading (our AP condition), consistent with the experimental results of the current study. Even higher stiffness values were recorded for free lateral loading or lateral loading with an axial constraint. These loads were applied quasi-statically so may

not be directly comparable to the results of the current study, but the benefit of simulation is the same "*ribs*" were utilized so the results are surely due to loading changes and not rib variation [47]. Unfortunately, to our knowledge, no comparative experimental rib or thorax data for the AP-L loading scenario as explored here exist.

More research to explore the effects and the optimal timing of combined loading to the thorax is necessary. Both 2D loading conditions utilized in this study were oversimplified in order to ensure repeatability and allow for direct comparisons within rib pairs. Rib angle, costal cartilage, and other anatomical variations of the thorax were not accounted for. Furthermore, the boundary conditions were over constrained and did not represent realistic belt or airbag interactions, which could possibly result in unrealistic fracture locations. It is unknown why two groups of fracture locations emerged in the AP-L condition (Fig. 3) as no relationships between fracture location or any structural properties were found. It may be that the rapid pot rotations at the vertebral or sternal rib ends caused shearing to occur at either end (see Fig. A13 for a comparison of typical bending in the AP versus flattening and possible shear in the AP-L condition). This makes extrapolation of these findings to potential differential effects of loading conditions on whole thoracic response and injury in more realistic scenarios difficult. Further investigation of the effects of combined loading on intact PMHS thoraces is necessary as a next step in understanding this complex issue. This work, at the single rib level and whole thorax, can also be expanded to analyze strain modes to better understand differences in fracture mechanisms between AP and AP-L type loading.

Small sample size (n=12 pairs) is a limitation of this exploratory study, and further research is necessary. However, an attempt was made to age-match between sexes and to have a large range of ages of adults represented in order to incorporate human variability into the sample while also attempting to control for a possible bias of age or sex in results.

V. CONCLUSIONS

A large difference in human rib structural response between AP only and AP-L tests was observed, with a more severe outcome that occurred sooner when the lateral constraint was incorporated into the loading scenario. This may have implications for injury outcomes in more realistic PMHS tests and real-world motor vehicle crash scenarios in terms of timing of restraint system deployment. More work should be done in this area to further explore potential effects of combined loading to the thorax. This research highlights the complexity of combined loading on human ribs that has not been investigated using experimental methods previously and provides important evidence to explore variability in whole thoracic response and injury severities in various scenarios with different combinations of restraints in physical and simulated experiments.

VI. ACKNOWLEDGEMENTS

We are grateful to the anatomical donors who provided these invaluable resources to further scientific inquiry. Thank you to Autoliv Research (Sweden) and the National Highway Traffic Safety Administration (VRTC, OH, USA) for sponsorship of various aspects of this research. The views contained within are those of the authors only and do not reflect opinions of sponsors or collaborators. Also, thanks to all students and staff of the Injury Biomechanics Research Center at The Ohio State University, especially Angela Harden, Randee Hunter, and Molly Tillis.

VII. REFERENCES CITED

[1] Kroell C, Schneider D, Nahum A. Impact tolerance and response of the human thorax. *Society of Automotive Engineers (SAE)*, 1971, Paper No. 710851.

[2] Kroell C, Schneider D, Nahum A. Impact tolerance and response of the human thorax II. *Society of Automotive Engineers (SAE)*, 1974, Paper No. 741187

[3] Nahum AM, Schneider DC, Kroell CK. Cadaver skeletal response to blunt thoracic impact. *Proceedings of 19th Stapp Car Crash Conference*, 1975, Paper No. 751150.

[4] L'Abbe RJ, Dainty DA, Newman JA. An experimental analysis of thoracic deflection response to belt loading. *Proceedings of IRCOBI Conference*, 1982, Cologne, Germany.

[5] Cesari D, & Bouquet R. Comparison of hybrid III and human cadaver thorax deformations loaded by a thoracic belt. *Stapp Car Crash Journal,* 1994, 38:65-76.

[6] Duma SM, Kemper AR, Stitzel JD, McNally C, Kennedy EA, Matsuoka F. Rib fracture timing in dynamic belt tests with human cadavers. *Clinical Anatomy*, 2011, 24(3):327-328.

[7] Kemper, A R, Kennedy, E.A, McNally, C, Manoogian, S J, Stitzel, J D, Duma, SM. Reducing chest injuries in automobile collisions: Rib fracture timing and implications for thoracic injury criteria. *Annals of Biomedical Engineering, 2011,* 39(8):2141-2151.

[8] Kent R, Lessley D, Sherwood C. Thoracic response to dynamic, non-impact loading from a hub, distributed belt, diagonal belt, and double diagonal belts. *Stapp Car Crash Journal*, 2004, 48:495-519.

[9] Albert DL, Beeman SM, Kemper AR. Assessment of thoracic response and injury risk using the Hybrid III, THOR-M, and Post-Mortem Human Surrogates under various restraint conditions in full-scale frontal sled tests. *Stapp Car Crash Journal*, 2018, 62:1-65.

[10] Kallieris D. Prediction of thoracic injuries in frontal collisions. *Proceedings of 16th International Technical Conference on the Enhanced Safety of Vehicles (ESV),* 1998, 2:1550-1563.

[11] Kang Y-S, Agnew AM, Hong CB, Icke K, Bolte IV JH. Elderly PMHS Thoracic Responses and Injuries in Frontal Impacts. *Proceedings of IRCOBI Conference*, 2017, Antwerp, Belgium.

[12] Kemper, AR, Beeman, SM, Porta DH, Duma SM. Non-censored rib fracture data using frontal PMHS sled tests. *Traffic Injury Prevention.* 2016, 17(1):131-140.

[13] Lessley DJ, Salzar R, et al. Kinematics of the thorax under dynamic belt loading conditions. *International Journal of Crashworthiness,* 2010, 15(2):175-190.

[14] Shaw G, Lessley D, et al. Small female rib cage fracture in frontal sled tests. *Traffic Injury Prevention*. 2017, 18(1):77-82.

[15] Lobdell TE, Kroell CK, Schneider DC, Hering WE, Nahum AM. Impact response of the human thorax. In *Human Impact Response*, 1973. pp. 201-245. Springer, Boston, MA.

[16] Morgan RM, et al. Thoracic trauma assessment formulations for restrained drivers in simulated frontal impacts. *Proceedings of the Stapp Car Crash Conference*, 1994, 38: Paper No. 942206.

[17] Eppinger RH, Marcus JH, Morgan RM. Development of dummy and injury index for NHTSA's thoracic side impact protection research program. *Society of Automotive Engineers (SAE)*, 1984, Paper No. 840885:983-1011.

[18] Kuppa S, Eppinger RH, McKoy F, Nguyen T, Pintar FA, Yoganandan N. Development of side impact thoracic injury criteria and their application to the modified ES-2 dummy with rib extensions (ES-2re). *Society of Automotive Engineers (SAE)*. 2003.

[19] Pintar FA, et al. Chestband analysis of human tolerance to side impact. *Society of Automotive Engineers (SAE)*. 1997, Paper No. 3612-3623.

[20] Viano DC. Biomechanical responses and injuries in blunt lateral impact. *Proceedings of 33rd Stapp Car Crash Journal,* 1989, 892432.

[21] Baudrit P, Petitjean A, Potier P, Trosseille X, Vallencien G. Comparison of the thorax dynamic responses of small female and midsize male post mortem human subjects in side and forward oblique impact tests. *Stapp Car Crash Journal,* 2014*,* 58:103-121.

[22] Trosseille X, Baudrit P, Leport T, Petitjean A, Potier P, Vallancien G The effect of angle on the chest injury outcome in side loading. *Stapp Car Crash Journal,* 2009*,* 53:403-419.

[23] Cavanaugh J, Walilko T, et al. Biomechanical response and injury tolerance of the thorax in twelve sled side impacts. *SAE Technical Paper (SAE)*, 1990, Paper No. 902307.

[24] Kallieris D, Mattern R, Schmidt G, Eppinger RH. Quantification of side impact responses and injuries. *Proceedings of 20th Stapp Car Crash Conference,* 1981, Paper No. 811009.

[25] Pintar FA, Yoganandan N, et al. Chestband analysis of human tolerance to side impact. *Proceedings of Stapp Car Crash Conference,* 1997, 41: Paper No. 973320.

[26] Riley PO, Arregui-Dalmases C, et al. Kinematics of the unrestrained vehicle occupants in side-impact crashes. Traffic *Injury Prevention*. 2012, 13(2):163-171.

[27] Acosta SM, Ash JH, Lessley DJ, Shaw CG, Heltzel SB, Crandall JR. Comparison of whole body response in oblique and full frontal sled tests. *Proceedings of IRCOBI Conference*. 2016.

[28] Lebarbe M, Potier P Baudrit P, Petit P, Trosseille X, Vallancien G. Thoracic injury investigation using PMHS in frontal airbag out-of-position situations. *Stapp Car Crash Journal,* 2005*,* 49:323-342.

[29] Rhule H, Suntay B, Herriott R, Amenson T, Stricklin J, Bolte JH. Response of PMHS to high- and low-speed oblique and lateral pneumatic ram impacts. *Stapp Car Crash Journal*, 2011, 55.

[30] Shaw J, Herriott R, McFadden J, Donnelly B, Bolte JH. Oblique and lateral impact response of the PMHS thorax. *Stapp Car Crash Journal*, 2006, 50:147-167.

[31] Yoganandan N, Pintar FA, Gennarelli TA, Martin PG, Ridella S. Chest deflections and injuries in oblique lateral impacts. *Traffic Injury Prevention,* 2008, 9(2):162-167.

[32] Yoganandan N, Pintar F, et al. Biomechanics of side impact: Injury criteria, aging occupants, and airbag technology. *Journal of Biomechanics*, 2007, 40(2):227-243.

[33] Sugaya H, Takahashi Y, et al., Development of a human FE model for elderly female occupants in side crashes. Proceedings of 26th International Technical Conference on *Enhanced Safety of Vehicles (ESV)*, 2019, Einthoven, Netherlands.

[34] Petitjean A, Baudrit P, Trosseille, X. Thoracic injury criterion for frontal crash applicable to all restraint systems. *Stapp Car Crash Journal,* 2003*,* 47:323-348.

[35] Bansal V, Conroy C, Chang D, Tominaga GT, Coimbra R. Rib and sternum fractures in the elderly and extreme elderly following vehicle crashes. *Accident Analysis and Prevention*, 2011, 43:661-665.

[36] Östling M, Saito H, Vishwanatha A, Ding C, Pipkorn B, Sunnevång C. Potential benefit of a 3+ 2 criss cross seat belt system in frontal and oblique crashes. Proceedings of IRCOBI Conference. 2017.

[37] Hu J, Boyle K, Fischer K, Schroeder A, Adler A, Reed MP. A New Prototype 4-Point Seatbelt Design to Help Improve Occupant Protection in Frontal Oblique Crashes. Proceedings of IRCOBI Conference. 2018: 114-124.

[38] Shurtz B, Agnew AM, Kang Y-S, Bolte JH. Application of scaled deflection injury criteria to two small, fragile females in side impact motor vehicle crashes. *Proceedings of World Congress of Biomechanics, SAE International*, 2018, 2018-01-0542.

[39] Agnew AM, Murach MM, et al. Sources of variability in structural bending response of pediatric and adult human ribs in dynamic frontal impacts. *Stapp Car Crash Journal*, 2018, 62:119-192.

[40] Charpail E, Trosseille X, Petit P, Laporte S, Lavaste F, Vallencien G. Characterization of PMHS ribs: A new test methodology. *Stapp Car Crash Journal*, 2005, 49:183-198.

[41] Li Z, Kindig M, et al. Rib fractures under anterior-posterior dynamic loads: Experimental and finite-element study. *Journal of Biomechanics*, 2010, 43:228-234.

[42] del Pozo de Dios, Kindig M, et al. Structural response and strain patterns of isolated ribs under lateral loading. *International Journal of Crashworthiness*, 2011, 16(2):169-180.

[43] Agnew AM, Dominguez VM, Sciulli PW, Stout SD. Variability of in vivo linear microcrack accumulation in the cortex of elderly human ribs. *Bone Reports*, 2017, 6:60-63.

[44] Yoganandan N, Pintar F. Biomechanics of human thoracic ribs. *Journal of Biomechanical Engineering*, 1998, 120:100-104.

[45] SAE. Instrumentation for impact test-part 1 – electronic instrumentation, J211/1. 2007. Warrendale, PA, USA.

[46] Kuppa S. Injury Criteria for Side Impact Dummies. 2004, Vol. 67. Washington, DC, National Transportation Biomechanics Research Center, National Highway Safety Administration, US DOT.

[47] Holcombe S, Wang C, Grotberg JB. The effect of rib shape on stiffness. *Stapp Car Crash Journal*, 2016, 60:11-24.

VIII. APPENDIX

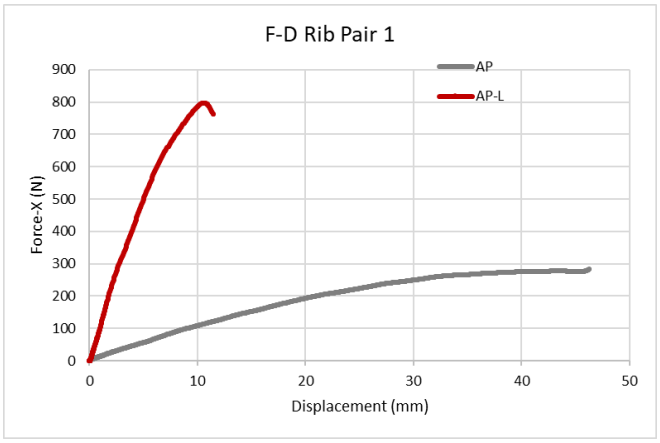

Fig. A1. Rib Pair 1 F_X-D Curves

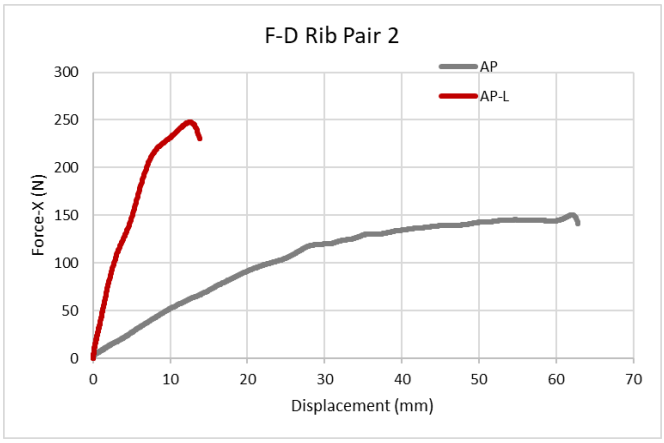

Fig. A2. Rib Pair 2 F_X-D Curves

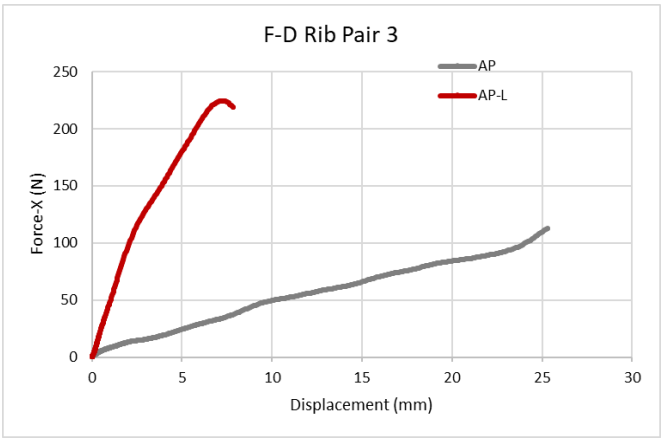

Fig. A3. Rib Pair 3 F_X-D Curves

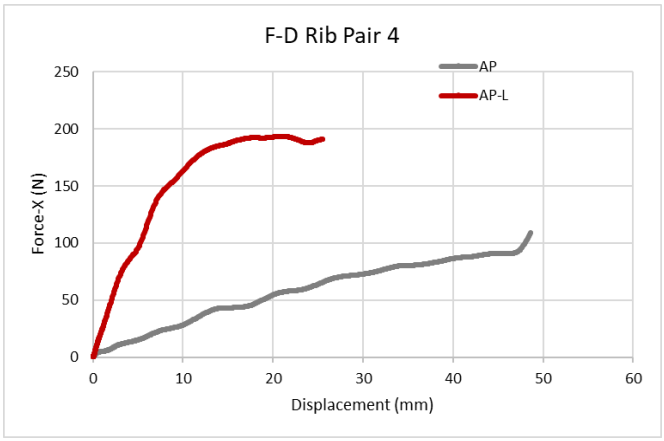

Fig. A4. Rib Pair 4 F_X-D Curves

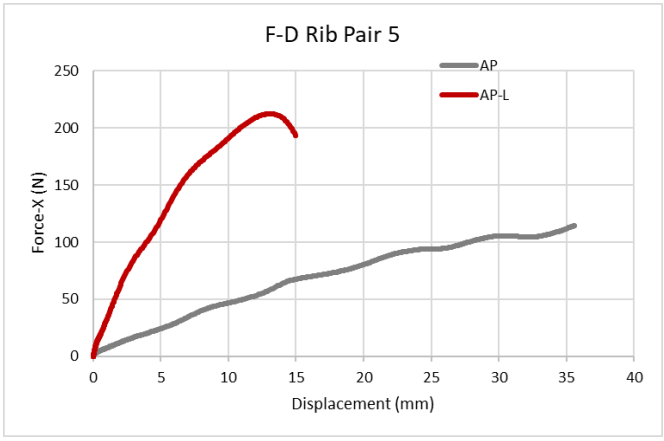

Fig. A5. Rib Pair 5 F_X-D Curves

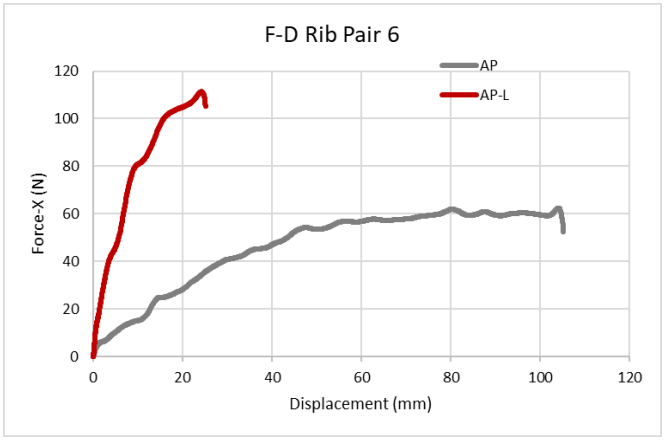

Fig. A6. Rib Pair 6 F_X-D Curves

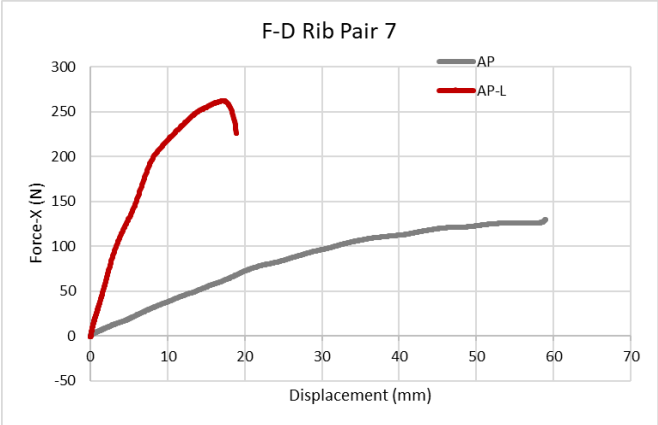

Fig. A7. Rib Pair 7 F_X-D Curves

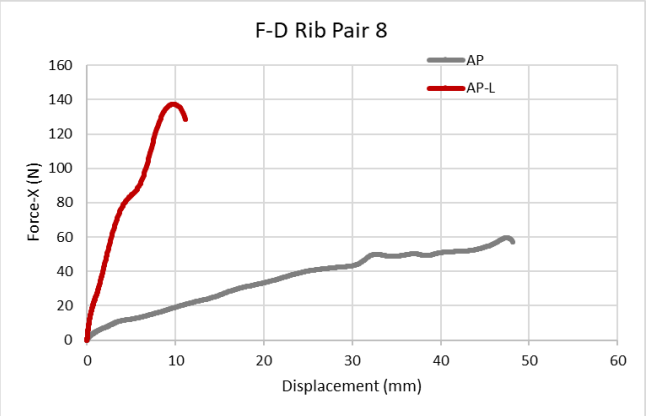

Fig. A8. Rib Pair 8 F_X-D Curves

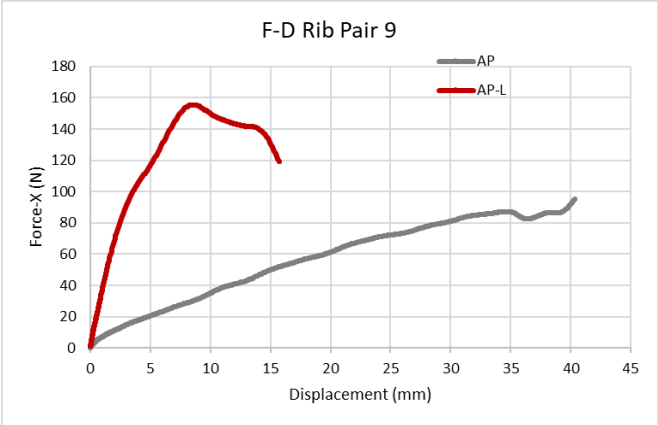

Fig. A9. Rib Pair 9 F_X-D Curves

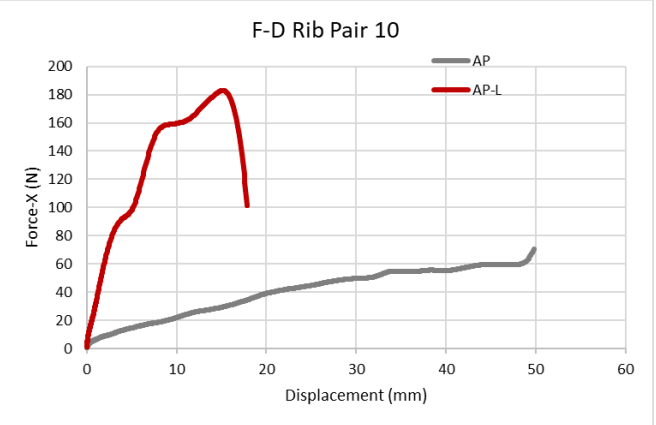

Fig. A10. Rib Pair 10 F_X-D Curves

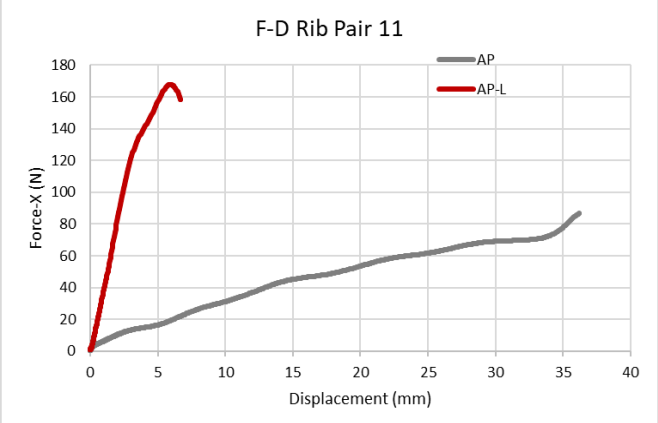

Fig. A11. Rib Pair 11 F_X-D Curves

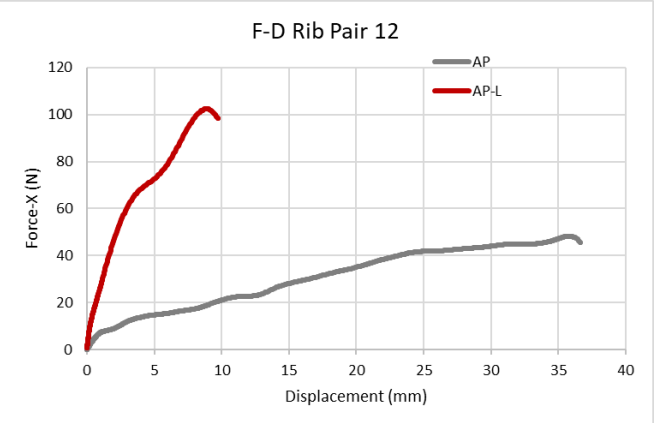

Fig. A12. Rib Pair 12 F_X-D Curves

TABLE AI
FRACTURE INFORMATION FOR RIB PAIRS

Pair	Loading Condition	Number of Fxs	Location of Fxs (%)
1	AP	1	90
	AP-L	1	66
2	AP	3	11, 47, 95
	AP-L	1	74
3	AP	1	65
	AP-L	1	71
4	AP	1	74
	AP-L	2	9, 93
5	AP	2	32, 86
	AP-L	2	14, 33
6	AP	2	39, 57
	AP-L	1	96
7	AP	1	84
	AP-L	1	6
8	AP	2	39, 83
	AP-L	1	89
9	AP	1	92
	AP-L	1	99
10	AP	1	74
	AP-L	1	18
11	AP	1	58
	AP-L	1	77
12	AP	3	39, 64, 81
	AP-L	1	70

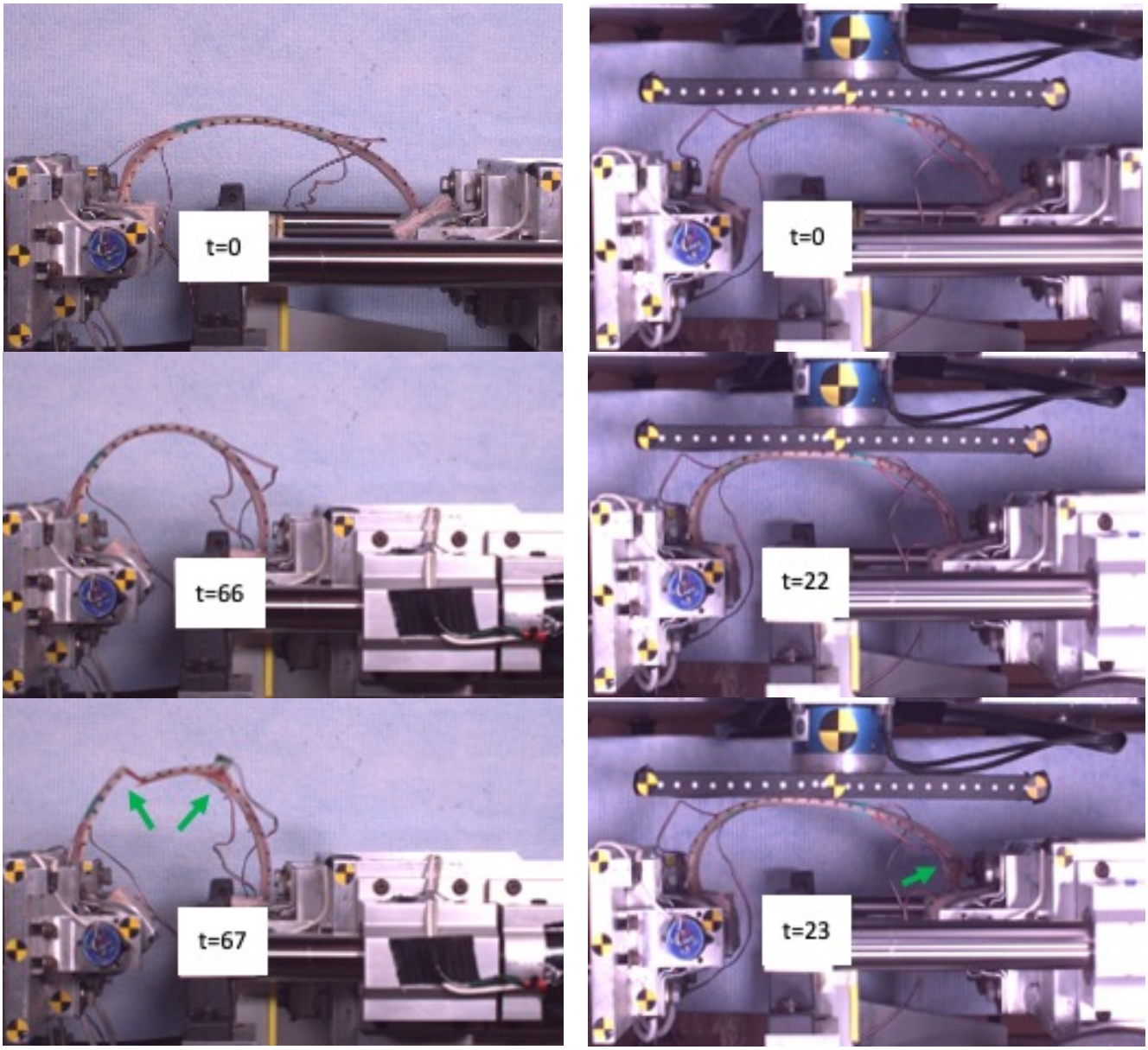

Fig. A13. Exemplar rib pair (Pair 6) comparing typical bending behavior in AP loading (left column) and a flattening effect from the rigid plate in AP-L (right column). Time (t) zero is in the top row, time just prior to fracture in the middle, and time of fracture in the bottom row. Times shown are in ms.